Combined ab Initio Computational and Statistical Investigation of a Model C−H···O Hydrogen Bonded Dimer as Occurring in 1,4-Benzoquinone

J. van de Bovenkamp,* J. M. Matxain, and F. B. van Duijneveldt

Theoretical Chemistry Group, Debye Institute, Utrecht University, Padualaan 14, 3584 CH, Utrecht, The Netherlands

T. Steiner

Institut für Kristallographie, Freie Universität Berlin, Takustrasse 6, D-14195, Berlin, Germany

Received: September 3, 1998; In Final Form: January 11, 1999

Ab initio molecular orbital calculations were performed on the C−H···O hydrogen bonded dimer pattern of the fragment O═C−C(═C)−H as occurring in 1,4-benzoquinone. The computations were combined with a statistical analysis of published crystal structures containing this dimer. For computational reasons, the dimer was approximated by dimers 1,4-benzoquinone−propenal and propenal−propenal. The optimal geometry obtained at the SCF+MP2 level of theory is very close to the mean geometry observed in crystals. The total binding energy ΔE at the optimal geometry is calculated as −17.9 kJ/mol. Each C−H···O hydrogen bond contributes about −6 kJ/mol, and the rest comes from stabilizing electrostatic interactions between the carbonyl groups. The potential energy surface has a broad shape at the minimum, allowing considerable geometric variations with only slight energetic disadvantages. The dimer geometries observed in crystals ($n = 53$) are all in the low-energy region of the potential energy surface. Only 4 of the 53 dimers have calculated ΔE values more than 3 kJ/mol above the global minimum. The dimer with the least favorable geometry has a ΔE value about 7.0 kJ/mol above the global minimum.

1. Introduction

Weak directional interactions of the type C−H···O are currently one of the main topics of hydrogen bond research,[1−5] in both the experimental and theoretical fields. The strengths of C−H···O hydrogen bonds, as judged from spectroscopic and geometric data, cover a wide range which overlaps with "normal" O/N−H···O hydrogen bonds for more acidic C−H donor types [such as C≡C−H, $CHCl_3$, $CH(NO_2)_3$],[6−8] and which merges with van der Waals interactions for the weakest C−H donors.[9,10] For alkynyl donors the spectroscopic effects of hydrogen bonding are still discernible at H···O distances of 2.9 Å,[11] suggesting that the interaction here comprises a significant long-range electrostatic component. As a consequence of their chemical diversity, the roles of C−H···O interactions in the solid state range from structure-determining to rather unimportant, depending on the nature of CH and O, and on the other interactions in play.

While the structural characteristics of C−H···O interactions are relatively well documented, energy-related questions are difficult to answer by studying structural and spectroscopic data alone. These questions include the following: What is the binding energy of a given C−H···O contact? To what extent does its geometry in the crystal deviate from the optimum geometry for the fragment in isolation, and how large is the energy needed to achieve this deformation? In a collection of similar C−H···O contacts, are contacts with a small deformation favored over such with large deformations? If this is the case, then it follows that these contacts can effectively optimize their geometries in the solid state, i.e., they play an active role in determining the crystal packing. Direct answers to these questions may be obtained by performing quantum chemical ab initio calculations on suitable (not too large) models for the interaction of interest. An accuracy of about 2 kJ/mol in the binding energies may currently be obtained routinely, provided one takes into account that these interactions may be rather weak.[12] We will show that it is possible to carry out the calculations in a step-by-step procedure that yields not only the total binding energy but also the size of its main components. In this way one may address the usually somewhat elusive questions regarding the nature of the interaction at hand.

SCHEME 1

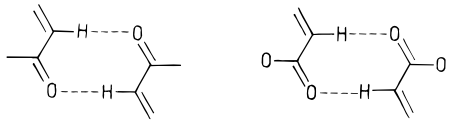

1 2

Our aim in this study is to characterize a chosen C−H···O interaction as fully as possible by performing a combined statistical and computational study. Many such studies have been performed previously on collections of *isolated* X−H···Y contacts captured from structural databases. However, there are distinct advantages in studying one of the well-defined *interaction patterns* that frequently occur in crystal structures.[13,14] One of the pioneering studies in this field was Leiserowitz' analysis of the related dimeric motifs **1** and **2** shown in Scheme 1.[15] They occur in many crystal structures of different kinds, with an archetypical example in 1,4-benzoquinone (Figure 1).[16] In this crystal structure, molecules are in one direction linked by pairs of mutual C−H···O hydrogen bonds in the dimer motif **1**, leading to formation of molecular ribbons. Neighboring ribbons are joined by lateral C−H···O hydrogen bonds, so that

10.1021/jp983607z CCC: $18.00
Published on Web 03/27/1999

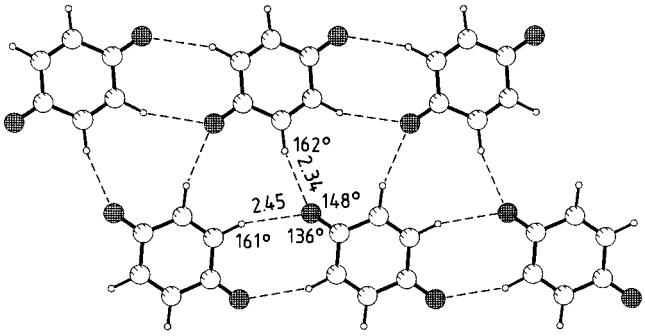

Figure 1. Molecular layer of crystalline 1,4-benzoquinone at room temperature, drawn using atomic coordinates from Trotter (distances in Å, angles in degrees).

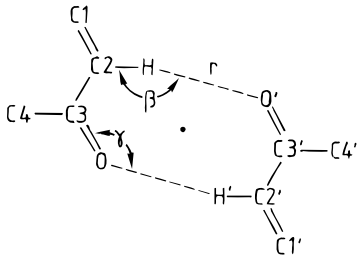

Figure 2. Search unit used in the statistical analysis, and atom labeling and geometric parameters used throughout in the text. Further definition: angle α = C3−C2···O′. The dot marks a center of symmetry.

all C−H groups of benzoquinone are engaged in hydrogen bonding. In the third dimension, the layers are stacked by optimizing aromatic−aromatic and carbonyl−carbonyl interactions. The dimer motif **1** is observed in many other crystal structures and may serve as a building block in the field of crystal engineering.[17] The motif linking the molecular ribbons is more specific to the particular structure of benzoquinone and is, therefore, of less general interest.

The advantages of studying such a pattern are the following. Since the pattern involves more than one hydrogen bond, its total impact on the crystal packing is relatively large, even if the individual bonds are weak. The geometry will be less perturbed by other interactions in the crystal, compared to that of an isolated hydrogen bond. The pattern can be characterized by a small set of geometrical parameters, leading to a good statistical coverage of the relevant coordinates and to a simplification of the computational study.

In the present work, we select dimer motif **1** as a suitable model system. Section 2 presents the results of a database search for this motif. The ab initio computational methods to obtain its interaction energy are described in section 3. A comparison between the results of the two techniques is presented in section 4. Finally, section 5 summarizes the conclusions.

2. Database Statistics

The statistical study is based on the organic crystal structures archived in the Cambridge Structural Database (CSD),[18] June 1997 update with 167 797 entries. Only ordered and error-free structures with *R* values less than 0.07 were used. H-atom positions were normalized [13] using the CSD default X−H bond lengths (C−H = 1.083 Å).

The search fragment used for the database analysis and the atom labeling scheme is shown in Figure 2. In the initial step of the analysis, intermolecular contacts of this type were retrieved with both H···O distances less than 3.0 Å. Because the majority of the contacts found is centrosymmetric, and because centrosymmetry leads to substantial simplification of the computational study, only the centrosymmetric contacts were retained. To filter out fragments with unrealistic H-atom positions, the covalent geometries of the relevant C−H bonds were inspected. Within the sample, the mean covalent angle C3−C2−H is found to be 117.9(4)° with σ = 5.4°. All fragments with this angle outside 118 ± 6° and also those with the torsion angle C4−C3−C2−H outside 180 ± 15° were considered as unrealistic and were excluded.

TABLE 1: Mean Geometries of C−H···O Interactions Between Molecular Fragments C═CH-CO-C[a]

	cyclic (motif **1**)[b]	noncyclic
n	53	69
H···O	2.47(2)	2.58(2)
C···O	3.53(2)	3.52(2)
C−H···O[b,c]	165.7(9)	148(2)
H···O═C	120(3)	130(3)

[a] Contacts must have (a) H···O < 3.0 Å, (b) C4-C3-C2···O′ < 20° (see Scheme 2); distances in Å and angles in degrees. [b] Only centrosymmetric arrangements. [c] The β-values obtained in the database search cannot be directly compared with the β used in the computational model, because in three-dimensional space, β is defined as a cone angle ≤ 180°.

For only very few of the obtained dimers are the two fragments exactly coplanar (because of the centrosymmetry, however, the planes of the fragments are parallel). In the following computational work, dimer **1** is approximated as planar, so it is imperative to consider only roughly planar arrangements also in the statistical analysis. As a compromise between the wishes to consider only geometries that are close to the theoretical model and to not omit a too large fraction of the experimental data, only those dimers **1** were retained which have a torsion angle C4−C3−C2−O′ < 20°. It is stressed that this does not mean that the less planar arrangements are "not linked by hydrogen bonds", but simply that they are not adequate representatives for the later theoretical model.

In the final step of data gathering, the dimers **1** passing the above criteria were individually inspected on the graphics display of an SGI workstation. Not only the dimers but also the carrier molecules were inspected for possible chemical inconsistencies (which do occur for a fraction of the data in the CSD) and for unrealistic intermolecular contacts.

Mean geometric parameters for the final 53 dimers **1** (in centrosymmetric and roughly planar geometry) are listed in Table 1, and distributions of some relevant geometric parameters are shown in Figures 3 and 4. The distributions of hydrogen bond distances H···O and C···O have mean values of 2.47(2) and 3.53(2) Å, respectively. The distribution of H···O distances, which is given in Figure 3a, falls practically to zero at long distances > 2.8 Å.

The hydrogen bond angle at the H-atom (β) peaks in the interval 160−170°, with a mean value of 165.7(9)°, Figure 3b. This is remarkably close to a linear angle: for the stronger C−H···O hydrogen bonds donated by terminal alkynes, the mean angle β is much lower, 152(2)°.[10] The near linearity is, presumably, a fortunate result of constraints within the cyclic geometry of **1**: because the O═C−C and C−C−H angles are ∼120°, a linear hydrogen bond happens to point exactly at the C═O lone pairs. This means that the preference of linearity at H and the preference for angles ∼120° at O═C support each other.

It is of some interest to see if it leads to major changes if the requirement of centrosymmetry is abandoned in the analysis. In a corresponding database search, only eight noncentrosymmetric dimers **1** were found which fulfill the quality and

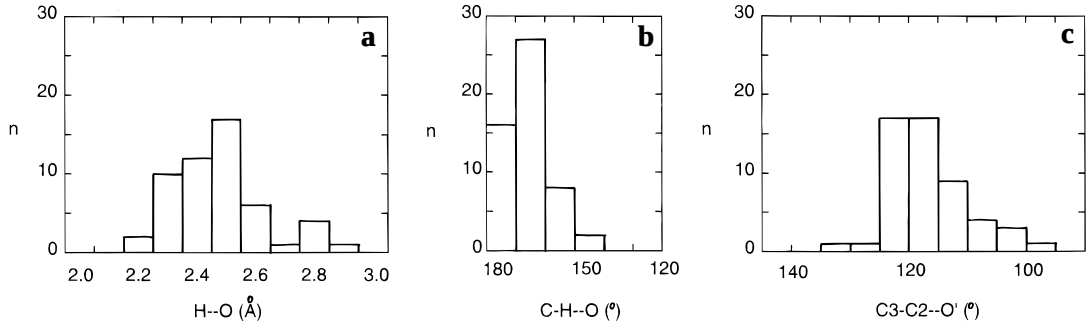

Figure 3. Distribution of the parameters (a) H···O, (b) C−H···O, and (c) C3−C2−O′ in dimers **1** in crystals.

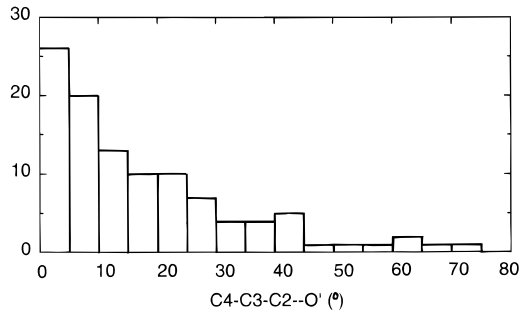

Figure 4. Distribution of torsion angles C4−C3−C2−O′ (absolute values) which measures the deviation of coplanarity of dimers **1** in crystals. Only dimers with this angle <20° were considered as "roughly planar" and included in the further analysis, and in Figure 3.

planarity criteria given above. In these dimers, the two hydrogen bond distances are unequal, and the differences between the two H···O separations range from 0.008 to 0.073 Å with the mean difference 0.048 Å. This means that centrosymmetric dimers **1** occur much more frequently in crystals than noncentrosymmetric ones, and for the latter, the dissymmetry is not very pronounced. Therefore, the restriction to the centrosymmetric case neglects only a minor fraction of the geometries that are experimentally observed.

An important point is to see whether the hydrogen bonds in dimer **1** have different average geometries than in the general case of C−H···O═C hydrogen bonds between the same fragments. Therefore, C−H···O contacts between two fragments of the kind shown in Figure 2 were retrieved from the CSD *with exception* of the cyclic motif **1**. All other quality and geometric criteria were retained. For 69 interactions of this kind, the mean geometries are listed in Table 1. The mean H···O distance is 0.11 Å longer than in **1**, the mean hydrogen bond angle β is more bent by 18°, and lone-pair directionality at the acceptor is less nicely obeyed. This shows that the cyclic dimer motif **1** has on the average a clearly better hydrogen bond geometry than noncyclic hydrogen bonds between the same molecular fragments.

3. Computational Study: Method

3.1 Components of the Interaction Energy. In weakly hydrogen-bonded systems, the dispersion energy is a nonnegligible contribution to the binding energy. Therefore, we performed the calculations at the SCF+MP2 level of theory. The SCF and MP2 interaction energies $\Delta E_{AB}(R)$, for a system AB separated by distance R, were calculated in the supermolecular approach and follow from

$$\Delta E_{AB}(R) = E_{AB}(R) - E_{A,DCBS}(R) - E_{B,DCBS}(R) \qquad (1)$$

where $E_{A,DCBS}(R)$ is the energy of monomer A, calculated in the complete basis set of the dimer (DCBS = dimer centered basis set). In (1), the counterpoise procedure of Boys and Bernardi [19] is used in order to avoid the basis set superposition error (BSSE).[20]

The SCF interaction energy ΔE(SCF) can be partitioned into a first-order energy $E^{(1)}$ and a second-order energy $E^{(2)}$.[21] $E^{(1)}$ contains Coulombic and exchange contributions associated with the unperturbed monomer wave functions and is obtained by subtracting the (DCBS) SCF monomer energies from the energy of the zeroth iteration in the dimer SCF calculation, in which the Schmidt orthogonalized (DCBS) SCF monomer wave functions are used as a start. $E^{(2)}$, called the second-order or deformation energy, contains induction, charge-transfer, and second-order exchange effects. It is the energy subsequently gained in the dimer SCF process.

The correlation interaction energy ΔE(MP2) contains, besides intramolecular correlation corrections on $E^{(1)}$ and $E^{(2)}$, the dispersion energy between uncorrelated monomers.[22] This dispersion energy also includes an exchange-dispersion contribution, since in the MP2 approach we use an antisymmetrized dimer wave function.

In the following, the total SCF plus MP2 interaction energy will be labeled ΔE, while ΔE(SCF) and ΔE(MP2) are used for its components. All calculations were performed using the ATMOL program package [23] and its local extensions SERVEC [24] and INTACAT.[25]

3.2. Basis Sets. To calculate interaction energies properly, the basis set should be able to describe the long-range as well as short-range terms of the interaction energy. To obtain accurate Coulombic, induction, and dispersion energies (the long-range terms), the electric multipole moments and polarizabilities must be accurately represented. Well-known energy-optimized basis sets such as 6-31G** and the singly polarized double-ζ (DZP) basis set have been found to yield poor results,[26] due to a lack of diffuse polarization functions. Therefore, we prefer so-called moment-optimized basis sets. In the course of this work, the following four basis sets were used.

The moment-optimized DZP′ basis set [27] has been advocated as the smallest basis set yielding reasonable electric properties. It is a (9, 5, 1/4, 1) → [4, 2, 1/2, 1] basis set of GTO's. This polarized double-ζ basis set contains a single set of polarization functions on each atom. The exponents of the polarization functions, $\alpha_p(H) = 0.15$ and $\alpha_d(C,O) = 0.25$, were optimized for a proper description of permanent dipole, quadrupole, and octupole moments and dipole polarizabilities.

The next basis set, ESP, is only slightly larger than DZP′. This basis set has an extended s-set ("ES") on C and O, taken from the extended (s,p) set in EZ. The EZ set for O is derived from DZ by replacing the most diffuse s function by two s functions and the two most diffuse p functions by three p functions.[28] A similar EZ set for C has been developed later by

van Mourik.[29] In contrast to basis DZP′, the exponents for the d polarization functions on C and O are $\alpha_d(C,O) = 0.50$. For H, the DZP′ basis set is used, with now $\alpha_p(H) = 0.387$.

Augmenting basis set ESP with one set of (s,p) bond functions, placed in the middle of the C−H···O hydrogen bond, we arrive at ESPB. The bond function exponents were chosen to be $\alpha_{s,p} = 0.60$. Bond functions have proved to be more effective in saturating the dispersion energy than atom-centered enlargements of the basis.[30]

Our largest basis set is called EZPPB. It is an extended ζ basis augmented with a double set of polarization functions and with the bond function set of ESPB. The EZ sets for C and O are taken from references 28 and 29, as described above. The exponents of the d polarization functions on oxygen and carbon are $\alpha_d(C,O) = 1.0$ and 0.25, while on hydrogen the p polarization function exponents have the values $\alpha_p(H) = 0.78$ and 0.19.[31] Due to the double set of polarization functions, EZPPB is expected to give the best results. Indeed, basis sets with a double set of polarization functions are known to give interaction energies for $(H_2O)_2$ that approach the SCF+MP2 basis set limit to about 1 kJ/mol.[21] We therefore take the results with basis set EZPPB as our reference values.

Throughout the calculations Gaussian atomic orbital basis sets with spherical harmonics for angular parts were used.

3.3 Geometries. In dimers analogous to that of **1** in 1,4-benzoquinone, the fragments are rarely exactly coplanar. However, in the experimental data set only dimers with relatively small nonplanarities have been considered, and this small noncoplanarity is neglected in the following calculations by keeping both monomers in one plane. In this case, the resulting centrosymmetric geometry depends only on two parameters, namely the H···O length R, and the C−H···O angle β (Figure 2). Moreover, since the interactions are expected to be weak, we did not perform any monomer geometry optimization, but used a fixed set of intramolecular distances and angles obtained from the X-ray crystal structure of benzoquinone.[16] Although in the experimental geometry the different C−C and C−H distances are not exactly equal, these were constrained to be equal in our calculations. The following intramolecular distances (in Å) were used: R(C−C) = 1.467, R(C═C) = 1.311, R(C═O) = 1.218, and R(C−H) = 1.086. The intramolecular C−C(═O)−C angle is 117.7 ° and the C−C−H angle is 121°.

If the complete 1,4-benzoquinone dimer is treated in our calculations, we encounter the problem that, even for the smallest basis set DZP′, the program limit of 255 basis functions is exceeded. In principle, this problem can be overcome by performing DIRECT-MP2 calculations, using for instance the GAMESS−UK program package.[32] However, we then lose the possibility of partitioning the interaction energy as described in section 3.1. We therefore followed a different strategy, perfoming calculations on the smaller systems 1,4-benzoquinone−propenal and the propenal dimer, using for propenal the same intramolecular distances and angles as for benzoquinone. It should be noted that for the system 1,4-benzoquinone−propenal, the basis set EZPPB is still too large (360 basis functions). The two models are shown in Figure 5. These systems should have C−H···O bond characteristics similar to those of the 1,4-benzoquinone dimer.

4. Computational Study: Results

4.1. Choice of Basis Set. Aim of the study is to calculate the interaction energy ΔE as a function of the parameters R and β. To choose an adequate basis set for this purpose, some preliminary calculations were performed on the propenal dimer (Figure 5). For convenience, we also define a (x,y) coordinate system, used throughout the calculations, in which the x-axis coincides with the corresponding H···O hydrogen bond axis when $\beta = 140°$. We first investigated ΔE as a function of R only, keeping the angle β at 140°. Results for ΔE as well as its components are summarized in Table 2, for all basis sets.

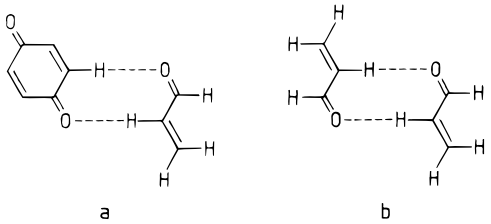

Figure 5. Molecular dimers used in the computational study: (a) 1,4-benzoquinone−propenal; (b) propenal−propenal.

TABLE 2: Propenal Dimer[a]

basis set	R	$E^{(1)}$	$E^{(2)}$	ΔE(SCF)	ΔE(MP2)	ΔE
DZP′	2.2672	7.9148	−8.2962	−0.3814	−5.5585	−5.9399
	2.4172	1.8843	−5.7318	−3.8475	−4.7630	−8.6105
	2.5672	−1.0317	−4.0881	−5.1198	−4.0819	−9.2017
	2.7172	−2.2642	−2.9950	−5.2592	−3.5118	−8.7710
	3.0172	−2.5174	−1.7154	−4.2328	−2.6311	−6.8639
	4.0172	−0.3462	−0.4061	−0.7524	−1.2351	−1.9875
	6.0172	0.6513	−0.0619	0.5882	−0.5559	0.0323
ESP	2.2672	10.6709	−7.9007	2.7702	−6.2764	−3.5062
	2.4172	4.1658	−5.3689	−1.2031	−5.0377	−6.2408
	2.5672	0.7759	−3.7709	−2.9950	−4.1025	−7.0975
	2.7172	−0.8635	−2.7260	−3.5895	−3.3979	−6.9873
	3.0172	−1.6809	−1.5287	−3.2096	−2.4561	−5.6657
	4.0172	−0.1812	−0.3600	−0.5412	−1.1942	−1.7354
	6.0172	0.6937	−0.0572	0.6365	−0.5400	0.0965
ESPB	2.2672	10.1322	−8.1273	2.0049	−7.3032	−5.2983
	2.4172	3.7945	−5.5400	−1.7455	−5.8380	−7.5834
	2.5672	0.5218	−3.8891	−3.3673	−4.7267	−8.0940
	2.7172	−1.0238	−2.8048	−3.8286	−3.8857	−7.7143
	3.0172	−1.7114	−1.5680	−3.2794	−2.7494	−6.0288
	4.0172	−0.1461	−0.3675	−0.5136	−1.2318	−1.7454
	6.0172	0.6986	−0.0574	0.6411	−0.5402	0.1009
EZPPB	2.2672	9.6165	−8.3318	1.2847	−8.8947	−7.6100
	2.4172	3.2710	−5.7055	−2.4345	−7.1383	−9.5728
	2.5672	0.0610	−4.0413	−3.9803	−5.7804	−9.7607
	2.7172	−1.4113	−2.9524	−4.3637	−4.7353	−9.0991
	3.0172	−1.9840	−1.7047	−3.6887	−3.2698	−6.9585
	4.0172	−0.1933	−0.4324	−0.6257	−1.2782	−1.9039
	6.0172	0.6896	−0.0665	0.6230	−0.4897	0.1334

[a] ΔE and its components for different distances R(H···O) and constant β (140°), for all basis sets. Energies in kJ/mol and distances in Å.

Comparing the total interaction energies first, significant differences between the four basis sets are found. Apparently, these are mainly due to differences in $E^{(1)}$ and ΔE(MP2). Indeed, $E^{(2)}$ is rather independent of the basis set used. Since $E^{(2)}$ is a relaxation term, it is always negative. It becomes more negative with decreasing R because induction and charge cloud overlap effects will be more pronounced at shorter distances. Concerning $E^{(1)}$, its behavior at short distances is entirely determined by the repulsive exchange contributions, while at larger distances electrostatic interactions are dominant. For the propenal dimer, a small positive $E^{(1)}$ value (∼0.7 kJ/mol), appears at R = 6.0172 Å for all basis sets. This repulsion is due to the dipole−dipole interaction between the two C═O groups. Taking the SCF C═O dipole moment to be 1.10 au[27] and assuming its origin to lie on the midpoint of the C═O bond (since for H_2CO this choice minimizes the size of the quadrupole moment[33]), we find a repulsion at this distance (about 1.8 kJ/mol) and, like $E^{(1)}$, the

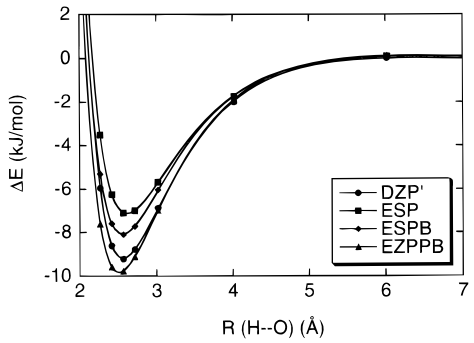

Figure 6. Potential energy curves for the propenal dimer, obtained by fitting $\Delta E(R)$ from Table 2 to the function $[c_1 \exp(c_2 R) + c_3/R^3 + c_4/R^6]$.

interaction changes sign as R decreases. However, to get quantitative agreement with $E^{(1)}$, the electrostatic contributions arising from the hydrogen bonds should be taken into account as well.

The DZP′ $E^{(1)}$ values are at all R significantly lower than those of the other basis sets. Since all basis sets give roughly the same value for the propenal (MCBS, SCF-level) dipole moment [μ(DZP′, ESP, ESPB, EZPPB) = 1.45, 1.46, 1.46, and 1.48 au, respectively], this might point to overestimation of other electric moments in DZP′ or to underestimation of short-range repulsion. However, we have not analyzed this aspect in further detail.

As expected, ESPB and EZPPB show significantly lower values for ΔE(MP2) than sets without bond functions, which is mainly the result of a more complete description of the dispersion interaction. For EZPPB, this trend is even more pronounced, since the set contains a double set of polarization functions. The lack of dispersion attraction in DZP′ may be explained by the fact that this set is known to underestimate dipole polarizabilities.[27]

The results for the R variation of ΔE, for all basis sets, are depicted in Figure 6. Concerning both the equilibrium distance and the well depth, the DZP′ potential energy curve is closer to the EZPPB curve than those for ESPB and ESP, pointing to a (partial) cancellation of errors for basis DZP′. Thus, although basis ESPB obviously gives better values for the separate interaction energy components than DZP′, basis set DZP′ seems well suited for calculating the potential curve. The equilibrium values for basis EZPPB are $R_{eq} = 2.52$ Å and $\Delta E(R_{eq}) = -9.85$ kJ/mol. For DZP′, R_{eq} is 0.04 Å longer, and $\Delta E(R_{eq})$ is about 0.80 kJ/mol less bonding. These values give lower limits of the basis set errors for DZP′.

To find out whether DZP′ would also be suitable for other β values, we investigated the motion perpendicular to the x-axis starting from the point $(x,y) = (2.55,0.0)$ Å, using basis sets DZP′ and EZPPB. The numerical results are collected in Table 3. Here, y denotes the perpendicular displacement and (R,β) defines the corresponding geometry. Again, the largest differences between the two sets occur for $E^{(1)}$ and ΔE(MP2). Figure 7 shows that the DZP′ curve again closely parallels the EZPPB curve in the whole range of y values, with a difference of 0.5 kJ/mol at the position of the minimum. The minima occur at the same position. On the basis of these results and considering the economy of calculations using DZP′, we regard basis set DZP′ as a good choice for calculating the grid of values $\Delta E(R,\beta)$.

4.2 Choice of System. Next, we investigated the effect of changing the system from the propenal dimer to benzoquinone−propenal. Calculations were performed by varying R and keeping β constant (140°), i.e., for $x = R$ and $y = 0$, using the ESPB basis set. Numerical results are given in Table 4. The potential energy curves are shown in Figure 8.

Comparing Tables 2 and 4, we find that for benzoquinone−propenal $E^{(1)}$ is significantly lower in the whole R range. At $R = 6.0172$ Å, $E^{(1)}$ has become negative (−0.12 kJ/mol). This can be explained by the fact that in benzoquinone−propenal, the second C═O group gives rise to a second dipole−dipole contribution to the interaction energy, which is negative for all the geometries considered. On the other hand, the effect of correlation, ΔE(MP2), is less negative than for the propenal dimer. This is because at the MP2 level the C═O dipole is 0.2 au less than at the SCF level, and so the C═O···C═O dipole−dipole attractions are reduced by about one-third after electron correlation is introduced.

The overall effect of changing from the propenal dimer to benzoquinone−propenal is a lowering of ΔE near the equilibrium geometry by about 2 kJ/mol, and shortening of the equilibrium H···O distance by 0.02 Å. Similar but smaller changes are expected if one were to make the further change to benzoquinone dimer, since two additional C═O···C═O interactions are introduced in this case. The short-range one is identical with that introduced by going from propenal dimer to benzoquinone−propenal, and stabilizes the interaction, while the other C═O···C═O interaction is more long-range and destabilizes the interaction. Considering that the errors we make in ΔE by using incomplete basis sets are at least 1 kJ/mol, and that the size of the benzoquinone dimer calculation would force us to use a program not providing energy partitioning, we select the benzoquinone−propenal system for generating a grid of ΔE values.

4.3. Calculation of a Grid of ΔE Values for Benzoquinone−propenal. For the calculation of the grid of ΔE values, the coordinate system (x,y) was used as defined in section 4.1. The origin is on the position of the acceptor oxygen atom of the benzoquinone unit, and the x-axis is defined by the condition that the H···O bond to propenal lies along x when $\beta = 140°$ (Figure 9). A Cartesian grid of geometries was constructed by moving the propenal unit in the (x,y) plane, the point (x,y) denoting the position of the propenal H atom. Because no rotation is performed, the centrosymmetry of the pattern is maintained.

Results for the total interaction energies ΔE, as well as the components $E^{(1)}$, $E^{(2)}$, and ΔE(MP2), at 35 different geometries are listed in Table 5. Subsequently, we generated a full two-dimensional potential energy surface by fitting an analytical potential energy function to these ΔE values. The following two polynomials in x and y were used:

$$V_1(x,y) = \sum_i \sum_j (x)^i (y)^j \quad \text{with} \quad (i+j) \le 4 \qquad (15 \text{ terms}) \tag{2}$$

$$V_2(x,y) = \sum_i \sum_j (x)^i (y)^j \quad \text{with} \quad (i+j) \le 5 \qquad (21 \text{ terms}) \tag{3}$$

The resulting equilibrium values for (R,β) and the binding energy ΔE, at both the SCF and SCF+MP2 levels of theory, are given in Table 6 for both V_1 and V_2. The accuracy of the two polynomials, expressed as the maximum deviation between V and ΔE, is also given. As expected, polynomial V_2 is found to be more accurate than V_1, at both the SCF and SCF+MP2 levels of theory. The fitting errors in R_{eq} and β_{eq}, as produced by V_2, are expected to be less than 0.005 Å and 0.5°, respectively.

TABLE 3: Propenal Dimer[a]

basis set	*y*	*R*	*β*	$E^{(1)}$	$E^{(2)}$	Δ*E*(SCF)	Δ*E*(MP2)	Δ*E*
DZP′	0.0	2.5501	140.59	−0.8009	−4.2437	−5.0447	−4.1573	−9.2020
	0.3	2.5676	147.30	−4.6087	−3.9979	−8.6066	−3.1402	−11.747
	0.6	2.6197	153.83	−7.2901	−3.5858	−10.876	−2.3655	−13.241
	0.9	2.7042	160.03	−9.0085	−3.0218	−12.030	−1.7780	−13.808
	1.2	2.8183	165.79	−9.8118	−2.3969	−12.209	−1.3396	−13.548
	1.5	2.9585	171.05	−9.8143	−1.8073	−11.622	−0.9995	−12.621
	1.8	3.1213	175.80	−9.2258	−1.3171	−10.543	−0.7209	−11.264
	2.1	3.3034	179.94	−8.2974	−0.9423	−9.2398	−0.4999	−9.7397
EZPPB	0.0	2.5501	140.59	0.3218	−4.1975	−3.8757	−5.9212	−9.7969
	0.3	2.5676	147.30	−3.6480	−3.9269	−7.5749	−4.7113	−12.286
	0.6	2.6197	153.83	−6.5708	−3.5026	−10.073	−3.7012	−13.775
	0.9	2.7042	160.03	−8.5343	−2.9427	−11.477	−2.8681	−14.345
	1.2	2.8183	165.79	−9.5451	−2.3342	−11.879	−2.1986	−14.078
	1.5	2.9585	171.05	−9.7061	−1.7680	−11.474	−1.6687	−13.143
	1.8	3.1213	175.80	−9.2343	−1.2986	−10.533	−1.2543	−11.787
	2.1	3.3034	179.94	−8.3866	−0.9405	−9.3271	−0.9336	−10.261

[a] Δ*E* and its components for the motion perpendicular to the *x* axis, for basis sets DZP′ and EZPPB. *y* denotes the perpendicular displacement and (*R*, *β*) defines the corresponding geometry. Energies in kJ/mol, distances in Å, and the angle *β* in degrees.

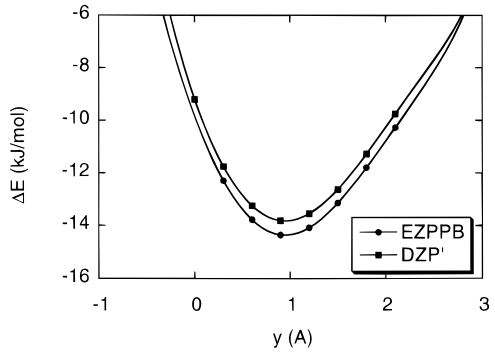

Figure 7. Δ*E* of the propenal dimer as a function of *y* (for constant *x*) for basis sets DZP′ and EZPPB.

TABLE 4: Δ*E* and Its Components for Different *R*(H···O) and Constant *β* (140°), but Now for the System 1,4-Benzoquinone−Propenal[a]

R	$E^{(1)}$	$E^{(2)}$	Δ*E*(SCF)	Δ*E*(MP2)	Δ*E*
2.2672	6.8485	−7.9118	−1.0633	−6.4598	−7.5231
2.4172	0.7788	−5.3493	−4.5705	−5.0298	−9.6002
2.5672	−2.2589	−3.7214	−5.9803	−3.9610	−9.9413
2.7172	−3.5951	−2.6590	−6.2541	−3.1466	−9.4007
3.0172	−3.9281	−1.4594	−5.3876	−2.0508	−7.4385
4.0172	−1.6009	−0.3261	−1.9270	−0.6720	−2.5990
6.0172	−0.1215	−0.0726	−0.0490	−0.2055	−0.3270

[a] Basis set ESPB. Energies in kJ/mol and distances in Å.

The electron correlation effects are seen to significantly affect the equilibrium parameters: R_{eq} is shortened by about 0.08 Å and *β* is enlarged by 6°. The equilibrium parameters yielded by the V_2 fit, $R = 2.429$ Å and $\beta = 176.8°$, agree reasonably well with the averages found in the database search (Table 6). In judging the quality of the agreement we must keep in mind that the use of better basis sets, and of the 1,4-benzoquinone dimer system rather than 1,4-benzoquinone−propenal would possibly shorten R_{eq} by about 0.05 Å to about 2.37 Å. This would be significantly shorter than the average obtained from the database. However, this average includes systems with nonlinear C−H···O angles and nonplanar geometries. Since in our calculations R_{eq} for $\beta = 140°$ equals 2.55 Å, rather than the 2.43 Å found near $\beta = 180°$, this is bound to have a lengthening effect on the average *R*.

A much more direct confrontation of theory and experiment is obtained by inspecting the way in which the database points are scattered in the (*x*,*y*) axis system. A two-dimensional contour

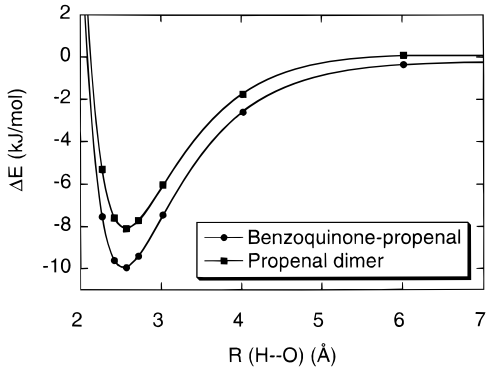

Figure 8. Comparison between the potential energy curves for the systems propenal dimer and 1,4-benzoquinone−propenal, obtained by fitting Δ*E*(*R*) from Tables 2 and 4 to the function $[c_1 \exp(c_2R) + c_3/R^3 + c_4/R^6]$. Basis set ESPB.

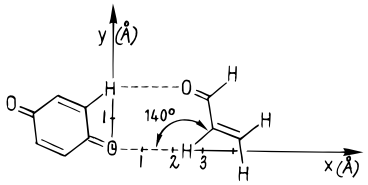

Figure 9. Definition of the (*x*,*y*) coordinate system for calculating the grid of Δ*E*(*x*,*y*) values. The origin is on the position of the acceptor oxygen atom of the benzoquinone unit, and the *x*-axis coincides with the corresponding H···O hydrogen bond axis when $\beta = 140°$. A point (*x*,*y*) specifies the position of the hydrogen bonded H-atom of the propenal molecule. The definition of the axis system is necessarily arbitrary.

plot of V_2 is shown in Figure 10. The dots in this Figure represent the geometries encountered experimentally (section 2). They were positioned on the basis of the C3−C2−O′ angles (α, see Figure 2) and the C···O lengths in a planar approximation of the experimental geometries. The plot shows a broad valley of low *V* values roughly along a circle with $R = 2.4$ Å around the acceptor oxygen atom at the origin of (*x*,*y*). In the optimal geometry, the H-bond is nearly linear ($\beta = 176.8°$) and the H-atom points at one of the C═O lone pairs, both aspects being typical of a normal H-bonding situation. The optimal H···O distance (2.43 Å), which would be shortened if a larger basis set were used, is significantly shorter than the 2.47 Å distance found in large basis SCF+MP2 calculations on the $(sp^2)C-H\cdots O(sp^3)$ bond in $C_2H_4\cdots OH_2$.[34] Likewise, the binding energy of −17.9 kJ/mol (for two H-bonds) is much lower than

TABLE 5: ΔE and Its Components, for the System 1,4-Benzoquinone−Propenal, at Different Points in the (x,y) Coordinate System of Figure 9[a]

x	y	R	β	$E^{(1)}$	$E^{(2)}$	ΔE(SCF)	ΔE(MP2)	ΔE
1.0000	2.00	2.2361	204.00	40.567	−15.951	24.616	−13.263	11.353
1.5172	2.00	2.5103	193.38	−2.3803	−5.5850	−7.9653	−6.0168	−13.982
1.6672	1.60	2.3107	184.49	−3.0060	−8.3037	−11.310	−5.1546	−16.465
1.6672	2.00	2.6038	190.75	−6.2629	−4.2391	−10.502	−4.6916	−15.194
1.8172	1.20	2.1776	174.00	1.2028	−11.570	−10.367	−4.2218	−14.589
1.8172	1.60	2.4212	181.93	−7.4586	−6.1175	−13.576	−4.0153	−17.591
1.8172	2.00	2.7022	188.31	−8.4608	−3.2498	−11.711	−3.6247	−15.336
1.9672	0.80	2.1236	162.70	5.5701	−12.918	−7.3479	−3.6941	−11.042
1.9672	1.20	2.3043	171.95	−5.6713	−8.0521	−13.723	−3.3629	−17.086
1.9672	1.60	2.5357	179.69	−9.9094	−4.5391	−14.449	−3.1015	−17.551
1.9672	2.00	2.8053	186.04	−9.5564	−2.5135	−12.070	−2.7528	−14.823
2.1172	0.80	2.2633	161.27	−3.3752	−8.6326	−12.008	−3.0495	−15.058
2.1172	1.20	2.4336	170.11	−9.3209	−5.6945	−15.016	−2.6222	−17.638
2.1172	1.60	2.6537	177.44	−11.026	−3.3978	−14.424	−2.3430	−16.767
2.1172	2.00	2.9125	183.94	−9.9348	−1.9618	−11.897	−2.0390	−13.936
2.2672	−0.60	2.3452	125.74	23.728	−8.4027	15.325	−8.0039	7.3211
2.2672	0.00	2.2672	140.57	4.9796	−8.0988	−3.1191	−4.6641	−7.7832
2.2672	0.40	2.3022	150.57	−2.2915	−7.4959	−9.7374	−3.2588	−12.996
2.2672	0.80	2.4041	160.00	−7.8936	−5.9202	−13.814	−2.4444	−16.258
2.2672	1.20	2.5652	168.46	−10.943	−4.0956	−15.039	−2.0057	−17.045
2.2672	1.60	2.7749	175.78	−11.281	−2.5689	−13.850	−1.7156	−15.566
2.2672	2.00	3.0233	181.98	−9.8563	−1.5436	−11.400	−1.4568	−12.857
2.4172	0.00	2.4172	140.57	−0.8328	−5.5518	−6.3846	−3.8956	−10.280
2.4172	0.40	2.4500	149.96	−6.2917	−5.1049	−11.397	−2.6690	−14.066
2.4172	0.80	2.5461	158.88	−9.8161	−4.1609	−13.977	−1.9359	−15.913
2.4172	1.20	2.6987	166.97	−11.340	−2.9953	−14.335	−1.4979	−15.833
2.4172	1.60	2.8987	174.07	−11.006	−1.9610	−12.967	−1.2195	−14.187
2.4172	2.00	3.1373	180.17	−9.4951	−1.2243	−10.719	−0.9967	−11.716
2.5672	0.00	2.5672	140.57	−3.5581	−3.9247	−7.4827	−3.2508	−10.734
2.5672	0.40	2.5982	149.42	−7.8692	−3.6015	−11.471	−2.1602	−13.631
2.5672	0.80	2.6889	157.87	−10.273	−2.9930	−13.266	−1.4790	−14.745
2.5672	1.20	2.8337	165.62	−11.032	−2.2257	−13.258	−1.0704	−14.328
2.5672	1.60	3.0250	172.50	−10.120	−1.5135	−11.634	−0.8060	−12.440
2.7172	0.00	2.7172	140.57	−4.6192	−2.8492	−7.4684	−2.7113	−10.180
2.8672	0.00	2.8672	140.57	−4.8133	−2.1154	−6.9287	−2.2488	−9.1775

[a] (R, β) defines the corresponding geometry. Basis set DZP′. Energies in kJ/mol, distances in Å, and the angle β in degrees.

TABLE 6: 1,4-Benzoquinone−Propenal[a]

level	polynomial	R_{eq}	β_{eq}	ΔE_{eq}	MD(ΔE)
SCF	V_1	2.508	173.9	−15.111	0.504
	V_2	2.512	170.8	−15.183	0.123
SCF+MP2	V_1	2.456	178.7	−18.095	0.540
	V_2	2.429	176.8	−17.945	0.131
database average		2.47(2)	174(1)[b]		

[a] Results for R_{eq} (in Å), β_{eq} (in degrees) and ΔE_{eq} (in kJ/mol), obtained by fitting the grid points to the polynomials V_1 and V_2, both at the SCF and SCF+MP2 level of theory. MD(ΔE) denotes the maximum deviation in the fit. The averaged results from the database search are also shown. [b] Estimation based on the mean value of α = 116.8°, neglecting the nonplanarity in the experimental data set. The average β (165.7°) quoted in Table 1 is not the appropriate β to compare to our calculated β_{eq}, for reasons given in footnote *c* of Table 1.

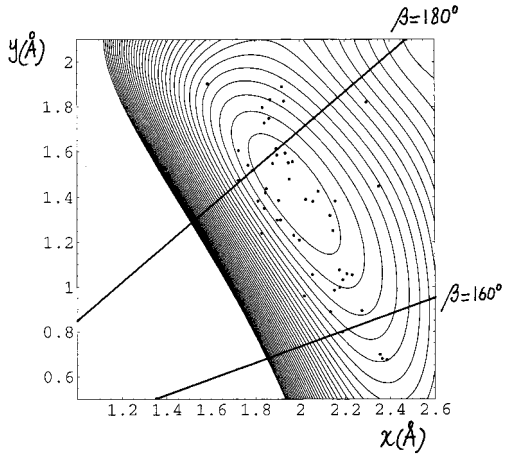

Figure 10. Contour map of the potential energy surface $V_2(x,y)$. The coordinate system is defined in Figure 9. The dots represent the geometries encountered in the database search. The lowest contour level corresponds to −17.5 kJ/mol, and the spacing between adjacent contour levels is 0.5 kJ/mol.

(twice) the $C_2H_4\cdots OH_2$ result of ΔE = −4.2 kJ/mol. These trends are partly caused by the larger acidity of the present C−H group compared to C_2H_4. In addition, about 5 kJ/mol of the extra stabilization originates from the C═O···C═O dipole interactions in the present system. At the optimal geometry, the C═O groups involved in the H···O contacts are antiparallel, with R ∼ 4.2 Å, yielding a dipole−dipole contribution of about −6 kJ/mol to $E^{(1)}$, and the more distant C═O···C═O interactions are also stabilizing. About a third of this dipolar stabilization is lost again in the MP2 step. Similar favorable C═O···C═O interactions are responsible for most of the binding in the formaldehyde centrosymmetric dimer studied by Ford et al. [35] as well as for that in the acetone dimer.[36] The frequent occurrence of stabilizing C═O···C═O interactions in crystal structures has only recently been described comprehensively.[37]

At the lower end of the valley (for y ∼ 0) the favorable C═O···C═O orientation is lost and $E^{(1)}$ accordingly rises from values of −11 kJ/mol near the optimum to less than −4 kJ/mol for $y \sim 0$. Part of the decrease is certainly due to the fact that the C−H···O bonds become increasingly bent. Finally, at the upper end of the valley ($x \sim 1.5$, $y = 2$) $E^{(1)}$ becomes rapidly less stabilizing, while $E^{(2)}$ and ΔE(MP2) become noticeably

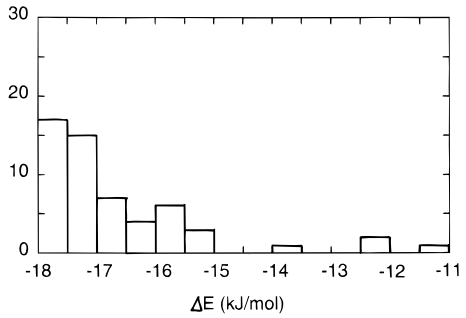

Figure 11. Density of experimental points between the contour lines of Figure 10 (in arbitrary units).

more stabilizing. This is because the C−H groups forming the H···O contacts approach each other until a large exchange repulsion starts to overtake $E^{(1)}$, as the sum of their van der Waals radii is reached.

Thus, motif **1** is seen to be strongly bound, partially by the two C−H···O bonds and partially by favorable C═O···C═O interactions. There is a wide range of favorable geometries accessible to this system, which is limited by C−H···H−C repulsion on one side and loss of C═O···C═O attraction on the other side.

To determine whether C−H···O hydrogen bonds are responsible for the packing in crystals containing motif **1**, an appropriate indicator should be found. The density of statistical points between two contour lines (see Figure 10) is a good criterion. The results depicted in Figure 11 show that the density of points rapidly decreases for ΔE values less negative than roughly −16 kJ/mol. This means that the C−H···O bonds in dimer **1** are strong enough to optimize their geometry in the interplay and competition with other intermolecular forces. The result is a structure-determining influence on the intermolecular architecture.

5. Conclusions

The statistical analysis of the C−H···O hydrogen bonded dimer motif **1** shows that this pattern of intermolecular interactions occurs frequently in crystals. The steric constraints within the motif are very favorable: hydrogen bond linearity and acceptor directionality are optimal for the same dimer geometry. In consequence, average angles at the H-atom and at the acceptor are far closer to optimal than for noncyclic CH···O═C bonds of the same fragments, and the mean H···O distance is significantly shorter. Motif **1** is an example where hydrogen bond geometries in a specific pattern are clearly better than in hydrogen bonds on average.

In the theoretical calculations, an optimal geometry of dimer **1** is obtained which is very close to the mean geometry observed in crystals [(H···O = 2.47 Å, β = 174°), given in Table 6]. This is a good indication that the theoretical results provide an adequate model of the experimental situation, despite the structural simplifications that had to be made. The calculated potential energy surface has a broad shape at the minimum that allows considerable distortions from optimal geometry with only slight energetic disadvantages: 49 of the 53 structures in the structural database have a ΔE value lower than −15 kJ/mol, i.e., less than 3 kJ/mol above the global minimum. This is most important in the context of molecular recognition and self-recognition: to be effective in molecular recognition and in solid state molecular architecture, dimer motif **1** must allow geometrical flexibility. In the solid state, such a motif can only rarely adopt the optimal geometry, but must normally adjust to a multitude of disturbing external influences. According to both the statistical and theoretical results, the C−H···O bonded dimer **1** appears to be sufficiently flexible in this sense. In this connection we note that, although ΔE for a 1,4-benzoquinone dimer is comparable to that of $(H_2O)_2$, the force constant in the R direction is only about two thirds that in $(H_2O)_2$, viz., 66 kJ/(mol Å^2) rather than 94 kJ/(mol Å^2).[31] For a single C−H···O contact of the type studied here one then expects a value near 33 kJ/(mol Å^2).

SCHEME 2

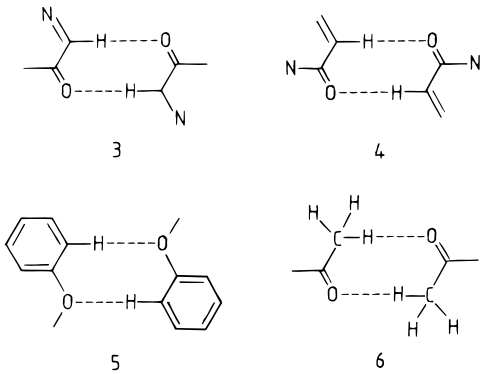

The total binding energy of the dimer at the optimum geometry is calculated to be $\Delta E = -17.9$ kJ/mol, but this value is likely to increase to about −20 kJ/mol if one were to use larger basis sets, and if one took the system 1,4-benzoquinone dimer rather than 1,4-benzoquinone−propenal. Thus ΔE is much the same as for a typical hydrogen bonding system like $(H_2O)_2$. However, the contributions making up ΔE are rather different. First, about −5 kJ/mol comes from C═O···C═O attraction. This leaves, in our calculations, about −6 kJ/mol for each C−H···O bond. The energy partitioning shows that in particular the $E^{(2)}$ term is much smaller than in $(H_2O)_2$ at its optimum (viz. about −2.5 kJ/mol versus −9 kJ/mol in $(H_2O)_2$ [31]). This reduction is a direct consequence of the H···O distance in C−H···O being much longer (2.4 Å) than that in O−H···O (1.95 Å), since the polarization and charge-transfer contributions in $E^{(2)}$ strongly diminish with increasing R. Moreover, in C−H···O the polarization of the acceptor by the X−H fragment will be much less than in O−H···O, on account of the relatively small polarity of the C−H bond.

To the extent that $E^{(2)}$ is a measure for the covalency of an X−H···Y contact we may conclude that the present C−H···O bonds are distinctly less covalent than the O−H···O bond in $(H_2O)_2$. In the same sense, the C−H···O bonds may be said to be more "van der Waals" like. Nevertheless, the directional properties of motif **1** as a whole are typical of a normal hydrogen-bonding interaction.

The observations on dimer **1** should be valid in a similar way also for structurally and chemically related arrangements. Examples are the long-known dimer **2**, but also dimers **3** and **4** (Scheme 2), which also occur in crystal structures. Even if the chemical situation is changed more dramatically, such as in dimers **5** and **6**, many of the general properties of **1** are possibly conserved.

Acknowledgment. T. S. thanks the Research Network "Molecular Recognition Phenomena" of the European Union for supporting two visits to Utrecht and the Minerva-Foundation (Munich) for awarding a fellowship to stay at the Weizmann Institute of Science in the laboratory of Professor Joel L. Sussman, where part of the manuscript was prepared.

References and Notes

(1) Steiner, T. *Cryst. Rev.* **1996**, *6*, 1.
(2) Steiner, T. *Chem. Commun.* **1997**, 727.
(3) Desiraju, G. R. *Acc. Chem. Res.* **1991**, *24*, 290.
(4) Desiraju, G. R. *Acc. Chem. Res.* **1996**, *29*, 441.
(5) Wahl, M. C.; Sundaralingam, M. *Trends Biol. Sci.* **1997**, *22*, 97.
(6) Bock, H.; Dienelt, R.; Schödel, H.; Havlas, Z. *J. Chem. Soc., Chem. Commun.* **1993**, 1792.
(7) Steiner, T.; Maas, J. van der; Lutz, B. *J. Chem. Soc., Perkin Trans. 2* **1997**, 1287.
(8) Kariuki, B. M.; Harris, K. D. M.; Philip, D.; Robinson, J. M. A. *J. Am. Chem. Soc.* **1997**, *119*, 12679.
(9) Steiner, T. *New J. Chem.* **1998**, 1099.
(10) Steiner, T.; Desiraju, G. R. *Chem. Commun.* **1998**, 891.
(11) Steiner, T.; Lutz, B.; Maas, J. van der; Schreurs, A. M. M.; Kroon, J.; Tamm, M. *Chem. Commun.* **1998**, 171.
(12) Hadzi, D. *Theoretical Treatments of Hydrogen Bonding*; Wiley: Chichester, 1997.
(13) Jeffrey, G. A.; Saenger, W. *Hydrogen Bonding in Biological Structures*; Springer: Berlin:, 1991.
(14) Bernstein, J.; Etter, M. C.; Leiserowitz, L.. In *Structure Correlation*; Bürgi, H.-B., Dunitz, J. D., Eds.; VCH: Weinheim, 1994; Vol. 2; pp 431−507.
(15) Leiserowitz, L. *Acta Crystallogr.* **1976**, *B32*, 775.
(16) Trotter, J. *Acta Crystallogr.* **1960**, *B13*, 86.
(17) Desiraju, G. R. *Angew. Chem., Int. Ed. Engl.* **1995**, *34*, 2311.
(18) Allen, F. H.; Kennard, O. *Chem. Des. Autom. News* **1993**, *8*, 1.
(19) Boys, S. F.; Bernardi, F. *Mol. Phys.* **1970**, *19*, 553.
(20) van Duijneveldt, F. B. Basis set superposition error. In *Molecular Interactions*; Scheiner, S., Ed.; Wiley: Chichester, 1997; pp 81−104.
(21) van Duijneveldt-van de Rijdt, J. G. C. M.; van Duijneveldt, F. B. Ab initio methods applied to hydrogen-bonded systems. In *Theoretical Treatments of Hydrogen Bonding*; Hadzi, D., Ed.; Wiley: Chichester, 1997; pp 13−47.
(22) Chalasinski, G.; Szczesniak, M. M. *Chem. Rev.* **1994**, *94*, 1723.
(23) Saunders: V. R.; Guest, M. F. ATMOL program package; SERC Daresbury Laboratory: Daresbury, UK.
(24) van Lenthe, J. H. SERVEC, ATMOL vector service program; University of Utrecht: Utrecht, The Netherlands, 1988.
(25) van Lenthe, J. H. INTACAT program package; University of Utrecht: Utrecht, The Netherlands, 1988.
(26) van Lenthe, J. H.; van Duijneveldt-van de Rijdt, J. G. C. M.; van Duijneveldt, F. B. *Adv. Chem. Phys.* **1987**, *69*, 521.
(27) van Duijneveldt-van de Rijdt, J. G. C. M.; van Duijneveldt, F. B. *J. Mol. Struct.* **1982**, *89*, 185.
(28) van Lenthe, J. H.; van Duijneveldt, F. B. *J. Chem. Phys.* **1984**, *81*, 3168.
(29) van Mourik, T. Correlated ab initio calculations on weakly bonded systems; University of Utrecht, The Netherlands, 1994.
(30) Burcl, R.; Chalasinski, G.; Bukowski, R.; Szczesniak, M. M. *J. Chem. Phys.* **1995**, *103*, 1498.
(31) van Duijneveldt-van de Rijdt, J. G. C. M.; van Duijneveldt, F. B. *J. Chem. Phys.* **1992**, *97*, 5019.
(32) Guest, M. F.; Fantucci, P.; Harrison, R. J.; Kendrick, J.; van Lenthe, J. H.; Schoeffel, K.; Sherwood, P. *GAMESS−UK*; Computing for Science (CFS) Ltd.: Daresbury, 1993.
(33) Vos, R. J.; Hendriks, R.; van Duijneveldt, F. B. *J. Comput. Chem.* **1990**, *11*, 1.
(34) Rovira, M. C.; Novoa, J. J.; Whangbo, M. H.; Williams, J. M. *Chem. Phys.* **1995**, *200*, 319.
(35) Ford, T. A.; Glasser, L. *J. Mol. Struct. (THEOCHEM)* **1997**, *398−399*, 381.
(36) Hermida-Ramón, J. M.; Ríos, M. A. *J. Phys. Chem. A* **1998**, *102*, 2594.
(37) Allen, F. H.; Baalham, C. A.; Lommerse, J. P. H.; Raithby, P. R. *Acta Crystallogr.* **1998**, *B54*, 320.